

# A Geometric Deformation Constrained Level Set Method for Structural Shape and Topology Optimization

S.Y. Wang<sup>1,2</sup>, K.M. Lim<sup>2,3</sup>, B.C. Khoo<sup>2,3</sup> and M.Y. Wang<sup>4</sup>

**Abstract:** In this paper, a geometric deformation constrained level set method is presented as an effective approach for structural shape and topology optimization. A level set method is used to capture the motion of the free boundary of a structure. Furthermore, the geometric deformation of the free boundary is constrained to preserve the structural connectivity and/or topology during the level set evolution. An image-processing-based structural connectivity and topology preserving approach is proposed. A connected components labeling technique based on the 4-neighborhood connectivity measure and a binary image is used for the present region identification. The corresponding binary image after an exploratory move of the free boundary at each time predicted by an explicit upwind finite difference scheme is first identified. Once a violation on structural connectivity and/or topology is encountered, removed components crucial to preserve the structural connectivity and/or topology are further identified and recovered to make the actual move properly connected. The geometric deformation is thus constrained and the structural connectivity and/or topology can be well maintained. Structural disconnectivity as well as topological changes during the evolution can be prevented. Shape optimization may be allowed for and topology optimization may become more robust. A bi-sectioning algorithm is used to handle the volume constraint and the fluctuations of the total volume can be

eliminated. The present method may be structural connectivity and/or topology preserving and volume conservative to generate monolithic feasible designs. The effectiveness of the present method is illustrated with numerical examples in minimum compliance design and compliant mechanism design.

**Keyword:** Level set method, topology optimization, shape optimization, geometric deformation, steepest gradient method, structural connectivity

## 1 Introduction

The level set method first introduced by Osher and Sethian [Osher and Sethian (1988)] has become increasingly popular recently. It is a simple and versatile numerical technique for computing and analyzing the motion of interfaces in two or three dimensions. The moving interfaces may easily develop sharp corners, break apart, merge together and even disappear to result in significant topological changes [Sethian (1999); Osher and Fedkiw (2002)]. The level set method has got a wide range of applications over the years [Osher and Fedkiw (2001); Osher and Paragios (2003); Tsai and Osher (2003)].

Recently, the level set methods have been applied to structural shape and topology optimization problems [Sethian and Wiegmann (2000); Allaire, Jouve, and Toader (2002); Wang, Wang, and Guo (2003); Allaire, Jouve, and Toader (2004)]. Sethian and Wiegmann [Sethian and Wiegmann (2000)] are among the first researchers to extended the level set method of Osher and Sethian [Osher and Sethian (1988)] to capture the free boundary of a structure on a fixed Eulerian mesh. The structural rigidity was maximized by using

---

<sup>1</sup> Corresponding author, Email: smaws@nus.edu.sg.

<sup>2</sup> Singapore-MIT Alliance, E4-04-10, 4 Engineering Drive 3, Singapore 117576.

<sup>3</sup> Department of Mechanical Engineering, National University of Singapore, Singapore 119260.

<sup>4</sup> Department of Mechanical and Automation Engineering, The Chinese University of Hong Kong, Shatin, NT, Hong Kong.

an *ad hoc* criteria based on the Von Mises equivalent stress. However, the classical shape sensitivity analysis [Sokolowski and Zolesio (1992)] was not introduced, which would be more suitable for the moving boundary-based optimization using the level set methods. Osher and Santosa [Osher and Santosa (2001)] investigated a two-phase optimization of a membrane modeled by a linear scalar partial differential equation (PDE). The moving free boundary was defined as the interface between two constituents occupying a given design domain. The level set method was combined with the classical shape sensitivity analysis, but the linear or nonlinear elasticity analysis of a structure was not involved. Allaire et al. [Allaire, Jouve, and Toader (2002, 2004)] proposed an implementation of the level set methods for structural topology optimization. The front velocity was derived from the classical shape sensitivity analysis by using an adjoint problem and the front propagation was performed by solving the Hamilton-Jacobi equation. Wang et al. [Wang, Wang, and Guo (2003, 2004)] established the velocity vector in terms of the shape of the moving free boundary and the variational sensitivity as a physically meaningful link between structural topology optimization and the versatile level set methods. The level set methods have been further developed in [Wang and Wang (2004b)] as a "color level set" method to address the issue of structural shape and topology optimization in a multi-material design domain. In [Wang and Wang (2005b)], the level set methods were further extended to a level set-based variational approach for the optimal shape and topology design of heterogeneous objects using a multi-phase level set model for digital image processing [Vese and Chan (2002)]. To overcome the limitation of the conventional level set methods in nucleation of new holes in the material domain, the classical topological derivatives [Sokolowski and Zochowski (2001)] were also exploited by some researchers [Burger, Hackl, and Ring (2004); Allaire, Gournay, Jouve, and Toader (2004); Allaire, de Gournay, Jouve, and Toader (2005); Amstutz and Andrä (2006)]. More recently, the use of radial basis functions was explored [Wang and Wang (2006b,c); Wang, Lim, Khoo, and Wang

(2007)] for structural shape and topology optimization using the level set methods to improve the computational efficiency and to reduce the probability of converging to a local minimum. In optimal synthesis of compliant mechanisms, the level set methods have been used as an effective tool for designing monolithic compliant mechanisms made of either single material [Allaire, Jouve, and Toader (2002, 2004); Chen, Wang, Wang, and Xia (2005); Mechkour, Jouve, Bidard, and Rotinat-Libersa (2006)] or multiple materials as an optimization of continuum heterogeneous structures [Mei and Wang (2004); Wang and Wang (2005b); Wang, Chen, Wang, and Mei (2005)].

In spite of the considerable advances recently achieved for shape and topology optimization using the level set methods, the undesirable connectivity issues resulting from the drastic topological changes and significant geometric deformations during the level set evolution were rarely addressed. The structural connectivity and/or topology may be destroyed due to the considerable geometric deformations, which may pose remarkable difficulty for structural shape and topology optimization. In the literature [Wang, Wang, and Guo (2003); Allaire, Jouve, and Toader (2004); Wang, Wang, and Guo (2004); Wang and Wang (2005b, 2006a,b,c); Wang, Lim, Khoo, and Wang (2007)], the level set methods have been successfully applied to shape and topological optimum of the minimum compliance design. The structural connectivity can be well maintained during the evolution since the minimum compliance design requires that the design become increasingly stiff with the evolution of the moving boundary. Hence, an explicit constraint on the structural connectivity would become unnecessary [Zhou and Wang (2006)]. However, the structural connectivity may not be generally preserved for applications different from the minimum compliance design. As shown in [Wang, Chen, Wang, and Mei (2005)], in compliant mechanism design using the level set methods, there is a strong tendency to destroy the structural connectivity in the geometric model and to develop the *de facto* hinge zones in the finite element (FE)-based physical model,

which may be due to the FE method adopted in structural analysis and the problem formulation used to obtain the design, as shown in the popular continuum optimal topology design of compliant mechanisms using the homogenization-based methods [Bendsøe and Sigmund (2003)]. The structural disconnection in the geometric model and the *de facto* hinge zones in the physical model would make the design questionable. An explicit constraint on the geometric deformation to preserve the structural connectivity becomes necessary. Nevertheless, further investigation into this issue was not taken into account by most researchers using the level set methods. The artificial spring model in continuum optimal topology design of compliant mechanisms using the homogenization-based methods to avoid the *de facto* hinge zones [Bendsøe and Sigmund (2003)] has been generally adopted [Allaire, Jouve, and Toader (2002, 2004); Mei and Wang (2004); Rahmatalla and Swan (2005); Wang and Wang (2005b); Wang, Chen, Wang, and Mei (2005); Mechkour, Jouve, Bidard, and Rotinat-Libersa (2006)]. However, this model may not guarantee the structural connectivity, or may generate a stiff rather than a flexible structure, depending on the the assumed stiffness of the artificial spring [Rahmatalla and Swan (2005)]. More recently, some preliminary study on the connectivity issue was reported in [Chen, Wang, Wang, and Xia (2005); Wang, Chen, Wang, and Mei (2005)]. Since the systematic connectivity analysis was not introduced, the preliminary study can neither eliminate the *de facto* hinges completely nor guarantee the smooth topology optimization, as illustrated in [Chen, Wang, Wang, and Xia (2005); Wang, Chen, Wang, and Mei (2005)]. The level set method has the potential to perform the mere boundary-based shape optimization due to the smoothness of the level set function (at least Lipschitz-continuous) [Osher and Fedkiw (2002); Tsai and Osher (2003)]. However, this potential may not be made full use of due to the lack of a topology preserving mechanism in the existing shape and topology optimization using the level set methods. In model reconstruction using the level set methods, Han et al. [Han, Xu, and Prince (2003)] developed a topology preserving geomet-

ric deformable model for brain cortical surface reconstruction. Nevertheless, the structural connectivity was not involved and only relatively simple topological changes were considered to simplify the analysis and the *de facto* hinge zones may not be eliminated due to the node-based connectivity measure. In structural shape and topology optimization, a volume constraint is usually involved to limit the use of material. The geometric deformation may thus be severely constrained. However, this volume constraint was either skipped [Allaire, Jouve, and Toader (2002, 2004); Wang and Wang (2006b)] or inappropriately handled due to the resulting fluctuations of the total volume [Osher and Santosa (2001); Wang, Wang, and Guo (2003); Wang and Wang (2005b); Wang, Chen, Wang, and Mei (2005); Wang and Wang (2006a)]. To guarantee a feasible design and the full use of the given material, the volume constraint must be handled properly.

The objective of the present study is to develop a geometric deformation constrained level set method to resolve these issues in shape and topology optimization using the level set methods. An image-processing-based structural connectivity preserving and/or topology preserving approach is proposed. The structural connectivity during the course of evolution can be guaranteed and the occurrence of *de facto* hinge zones in the FE-based physical model can be prevented. Furthermore, the structural topology can be preserved to perform the boundary-based shape optimization only. The volume constraint can be effectively handled to make full use of the given material by the bi-sectioning algorithm. Numerical examples in two dimensions (2D) that are widely investigated by many other researchers are chosen to demonstrate the distinctive effectiveness of the present level set method for structural shape and/or topology optimization.

## 2 A Geometric Deformation Constrained Level Set Method

### 2.1 Hamilton-Jacobi Equation

The level set method is a powerful and versatile numerical technique. In the standard level set

method first introduced by Osher and Sethian [Osher and Sethian (1988)], the interface (or moving boundary) is embedded into a higher-order (one dimension higher) level set function  $\Phi(\mathbf{x})$  as the zero level set  $\{\mathbf{x} \in \mathbb{R}^d \mid \Phi(\mathbf{x}) = 0\}$  ( $d = 2$  or  $3$ ). The implicit scalar level set function  $\Phi(\mathbf{x})$  has the following properties:

$$\begin{aligned} \Phi(\mathbf{x}) = 0 &\iff \forall \mathbf{x} \in \partial\Omega \cap \mathcal{D} \\ \Phi(\mathbf{x}) < 0 &\iff \forall \mathbf{x} \in \Omega \setminus \partial\Omega \\ \Phi(\mathbf{x}) > 0 &\iff \forall \mathbf{x} \in (D \setminus \Omega) \end{aligned} \quad (1)$$

where  $\mathcal{D} \subset \mathbb{R}^d$  is a fixed design domain in which all admissible shapes  $\Omega$  (a smooth bounded open set) are included, i.e.  $\Omega \subset \mathcal{D}$ . Figure 1 displays that a 2D design can be embedded into a 3D level set function  $\Phi(\mathbf{x})$ , which is a signed-distance function for this case.

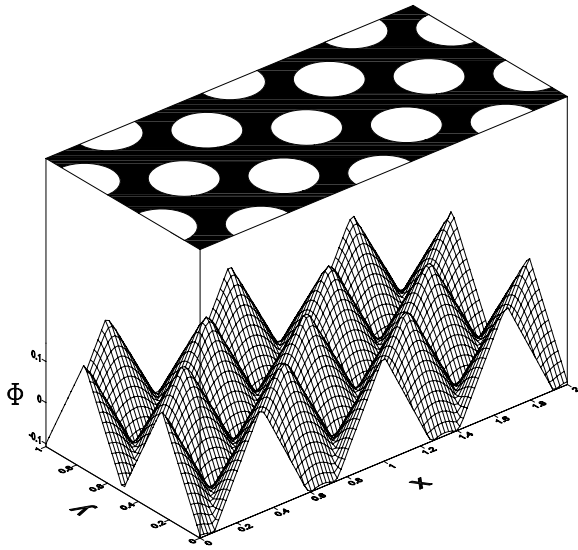


Figure 1: Level set description of a 2D design.

To let the level set function dynamically change with time, i.e.  $\Phi(\mathbf{x}) = \Phi(\mathbf{x}, t)$ , where  $t$  is the pseudo time, a continuous normal velocity field  $v_n(\mathbf{x}, t)$  should be provided. In the present shape and topology optimization, this velocity field is determined by a steepest gradient method, which will be discussed in the following section. The evolution of the interface or moving boundary can be obtained by solving the following Hamilton-Jacobi equation [Sethian (1999); Osher and Fed-

kiw (2002)]:

$$\frac{\partial \Phi}{\partial t} + v_n |\nabla \Phi| = 0, \quad \Phi(\mathbf{x}, 0) = \Phi_0(\mathbf{x}) \quad (2)$$

where  $\Phi_0(\mathbf{x})$  embeds the initial position of the interface, and the relationship between the normal velocity  $v_n(\mathbf{x}, t)$  and the velocity  $v(\mathbf{x}, t)$  is:

$$v_n = v \cdot n \quad (3)$$

in which  $n$  is the outward normal defined by

$$n = \frac{\nabla \Phi}{|\nabla \Phi|} \quad (4)$$

Usually, the Hamilton-Jacobi PDE (2) is solved to evolve the interface by using a capturing Eulerian approach based on an explicit upwind finite difference scheme [Osher and Fedkiw (2002)]. The solving procedure requires appropriate choice of the upwind schemes, reinitialization algorithms and extension velocity methods [Sethian (1999); Osher and Fedkiw (2002)]. Furthermore, the timestep size must be sufficiently small to satisfy the CFL condition ( $\text{CFL} \leq 1$ ) to ensure the convergence of the solution [Sethian (1999); Osher and Fedkiw (2002)]. In this study, a second-order ENO (essentially non-oscillatory) upwind scheme is used for the propagation of the moving boundary and a third-order reinitialization algorithm is adopted to minimize the numerical diffusion around the location of the original interface [Osher and Fedkiw (2002); Tsai and Osher (2003)], and an aggressive CFL number of  $\text{CFL} = 0.9$  is used to drive a fast convergence speed. Reinitialization is only performed as an auxiliary step. A natural extension velocity method is to be presented in the following section to preserve the simplicity of a level set method. As shown in [Sethian and Wiegmann (2000); Osher and Santosa (2001); Allaire, Jouve, and Toader (2004); Wang, Wang, and Guo (2003)], drastic topological changes and significant geometric deformations of a level set model can be achieved. However, as aforementioned, the geometric deformation may even hinder further applications of the level set methods in structural shape and topology optimization.

In the present study, a geometric deformation constrained level set method is developed. The propagation of the interface at each time  $t$  predicted by the explicit upwind finite difference scheme [Osher and Fedkiw (2002)] is taken as an exploratory move of the interface only. The exploratory move will be accepted as an actual move only if the connectivity requirements are satisfied. Otherwise, the motion of parts of the interface crucial to preserve the connectivity will be constricted after an image-processing-based connectivity analysis is performed. More details are to be given in the following sub-sections.

## 2.2 A Structural Connectivity Preserving Level Set Method

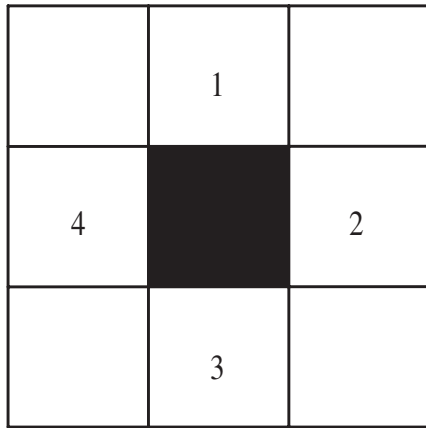
In this study, a structural connectivity preserving level set method based on an image-processing technique is first proposed. In image processing for a 2D problem [Jahne (1997)], either a 4-neighborhood connectivity, where only vertical and horizontal directions can be followed, or a 8-neighborhood connectivity, where horizontal, vertical and diagonal directions are allowed, can be used, as shown in Fig. 2. To determine the structural connectivity more effectively, the 4-neighborhood connectivity is employed in the present study. Since the undesirable patches of checkerboard patterns, within which the density of the material assigned to contiguous finite elements varies in a periodic fashion similar to a checkerboard consisting of alternating solid and void elements [Bendsøe and Sigmund (2003)], will not be considered as appropriately connected in the 4-neighborhood connectivity, the occurrence of checkerboard patterns is actually prohibited in a structurally connected design. Furthermore, the edge connection imposed by the 4-neighborhood connectivity, rather than the node connection permitted by the 8-neighborhood connectivity, may prevent the occurrence of weak connections such as *de facto* hinges during the course of evolution [Wang, Tai, and Wang (2006)].

Moreover, in image processing [Jahne (1997)], region identification is indispensable for region description since extracting and labeling of vari-

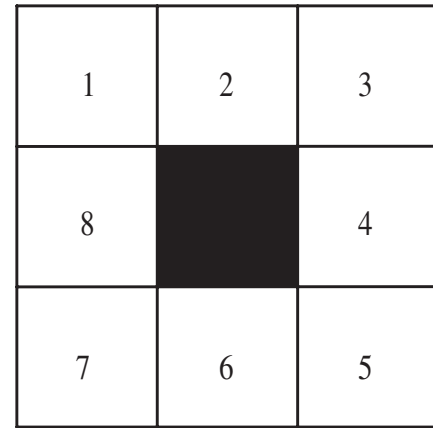
ous disjoint and connected components in an image is central to many automated image analysis applications. In this study, the connected components labeling approach [Jahne (1997); Chang, Chen, and Lu (2004)] is used for region identification. The connected components labeling approach scans an image and groups its pixels into components based on pixel connectivity. Once all groups have been determined, each pixel is labeled with a unique (integer) number according to the component it was assigned to. With this labeling, the number of connected regions and their relative areas can be readily obtained with a simple inspection of the labeled image's histogram [Wang and Wang (2005a)]. The connected components labeling approach can work on binary or gray-level images and different measures of connectivity. In the present structural connectivity analysis, only binary input images and the 4-neighborhood connectivity measure are taken into account. Figure 3 displays the region identification procedure for a 0-1 topological design using the connected components labeling approach. After obtaining the bit-array representation of the input 0-1 design, the connected components labeling can be performed. The resulting labelled connected components can be expressed as

$$C^{\text{lab}} = \{c^1, c^2, \dots, c^i, \dots, c^N\} \quad (5)$$

where  $C^{\text{lab}}$  is the set of all labelled connected components,  $c^i$  the  $i$ -th labelled connected component, and  $N$  the total number of labelled connected components. For this case, it has been identified that  $N = 4$  and  $c^2$  is the structurally connected component, which has the load bearing capacity when the left end of the design domain is fixed and a concentrated load is applied at the centre of the right free end, as shown in Fig. 3(d). As expected, a 0-1 structurally connected design must have one structurally connected component. To provide the discrete 0-1 design for region identification, in this study, the fixed FE discretized design domain  $\mathcal{D}$  is approximated as a black-and-white digital image, or binary image. Each element is analogously considered as one pixel and its color is represented by a binary variable only, where white is void and black is solid ma-

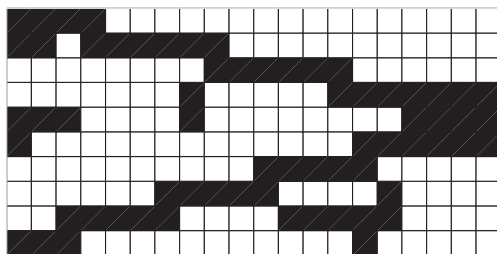


(a) 4-neighborhood connectivity

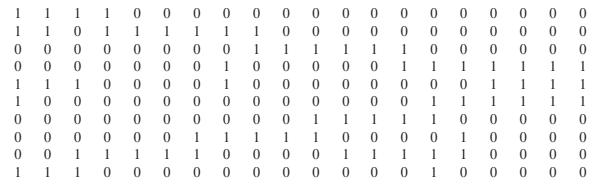


(b) 8-neighborhood connectivity

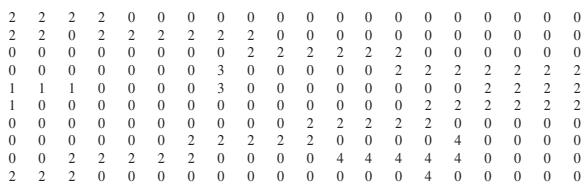
Figure 2: Connectivity measures for a 2D problem.



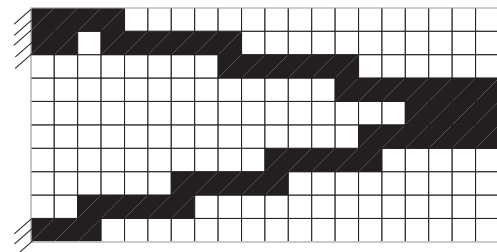
(a) Original 0-1 design



(b) Bit-array representation



(c) Connected components labeling



(d) Identified structurally connected component

Figure 3: Region identification using connected component labeling.

material. It is assumed that the elements with intermediate values can be neglected since these elements may result in the unreliable weak connections such as the *de factor* hinges during the level set evolution and the removal of them for region identification would greatly simplify the connectivity analysis without destroying the reliable structural connectivity. Hence, only the approximated design strictly comprising discrete 0-1 ele-

ments are taken into account in the present image-processing-based connectivity analysis. Figure 4 displays the procedure to obtain the binary image of an admissible design for a compliant mechanism design problem. It can be seen that the binary image of an admissible design that transmits the applied forces from the specified input region (port) to the output region (port) by elastic deformation can be readily obtained by removing those

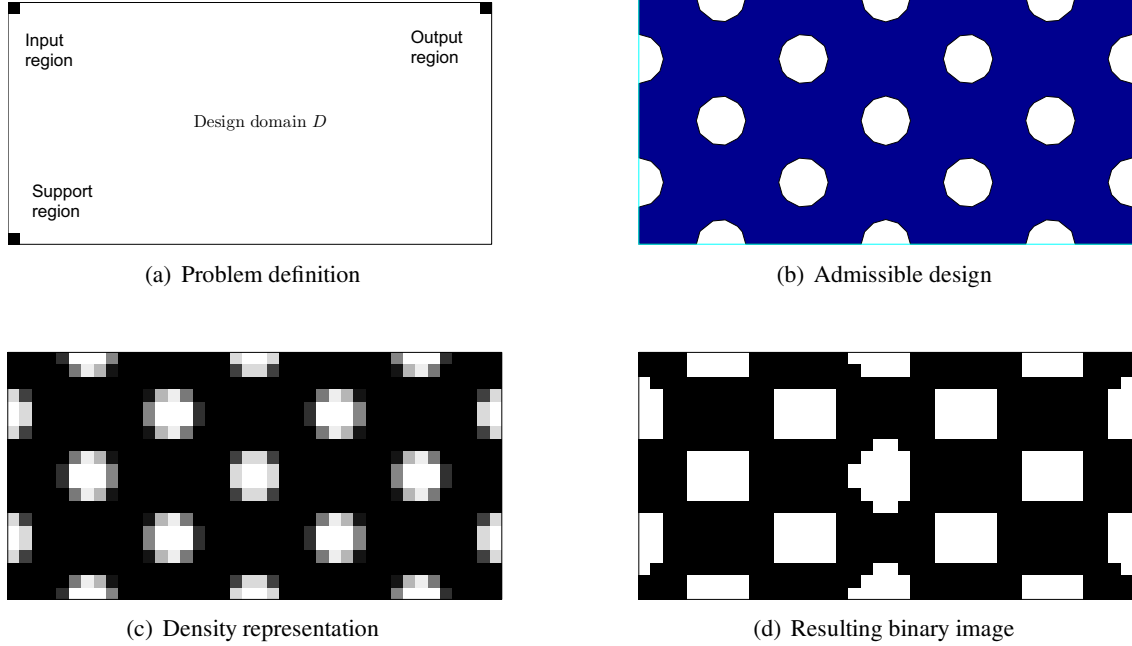


Figure 4: Binary image of an admissible design.

elements with intermediate densities.

A structural connectivity preserving level set method based on the image-processing technique can then be developed. As aforementioned, the propagation of the moving boundary at each time  $t$  predicted by using an explicit upwind finite difference scheme [Osher and Fedkiw (2002)] to solve the Hamilton-Jacobi PDE (2) is only taken as an exploratory move. This exploratory move will be considered acceptable as an actual move only if the binary image  $\mathfrak{I}_{\text{exp}}$  of the resulting design is structurally connected. If there is no structurally connected component among all the labelled connected components  $C_{\text{exp}}^{\text{lab}}$ , the binary image will be identified as structurally disconnected and thus the exploratory move cannot be accepted as an actual move. Hence, to maintain the structural connectivity, we need to further analyze the removed solid elements during the exploratory move. The set of removed elements  $C_{\text{rem}}$  can be obtained as

$$C_{\text{rem}} = \mathfrak{I}_t \setminus (\mathfrak{I}_{\text{exp}} \cap \mathfrak{I}_t) \quad (6)$$

by comparing the binary images  $\mathfrak{I}_t$  and  $\mathfrak{I}_{\text{exp}}$  before and after the exploratory move respectively. Furthermore, the connected components of  $C_{\text{rem}}$

can be labelled as  $C_{\text{rem}}^{\text{lab}}$ :

$$C_{\text{rem}}^{\text{lab}} = \{c_{\text{rem}}^1, c_{\text{rem}}^2, \dots, c_{\text{rem}}^i, \dots, c_{\text{rem}}^{NR}\} \quad (7)$$

where  $NR$  is the total number of the connected components of the removed solid elements. The effect of each component  $c_{\text{rem}}^i$  on the structural connectivity of the binary image  $\mathfrak{I}_t$  can be obtained by gradually removing the components identified as irrelevant to the structural connectivity from  $\mathfrak{I}_t$  using the connected components labeling approach [Jahne (1997); Chang, Chen, and Lu (2004)] again. The remaining components  $C_c^{\text{lab}} \subset C_{\text{rem}}^{\text{lab}}$  must be crucial to maintain the structural connectivity and thus cannot be removed during the exploratory move, which can be expressed as

$$C_c^{\text{lab}} = \{c_c^1, c_c^2, \dots, c_c^i, \dots, c_c^{NC}\} \quad (8)$$

where  $NC$  is the total number of the crucial components ( $NC \leq NR$ ). These crucial components should be recovered in the binary image  $\mathfrak{I}_{\text{exp}}$  and thus the resulting binary image after the exploratory move should be modified as  $\tilde{\mathfrak{I}}_{\text{exp}}$ :

$$\tilde{\mathfrak{I}}_{\text{exp}} = \mathfrak{I}_{\text{exp}} + C_c^{\text{lab}} \quad (9)$$

The recovery of the crucial components may be equivalent to setting zero velocities at the corresponding local grid points to restrict their movement during the level set evolution. Hence, the decrease of the objective function for shape and topology optimization can be well maintained due to the steepest gradient method [Osher and Santosa (2001); Wang, Wang, and Guo (2003); Allaire, Jouve, and Toader (2004)] adopted and the relatively small movement of the free boundary (less than one grid size) at a single timestep constricted by the CFL condition [Sethian (1999); Osher and Fedkiw (2002)]. Therefore, the optimality condition can be well kept and the numerical instabilities can be avoided.

Comparing with the topology preserving geometric deformable model for brain cortical surface reconstruction in model reconstruction using the level set methods [Han, Xu, and Prince (2003)], the present method can not only preserve the structural connectivity, but also well maintain the decrease of the objective function due to the present zero velocities rather than the  $\Phi$  values of the non-simple grid points with changed signs only [Han, Xu, and Prince (2003)] and prevent the occurrence of weak connections such as the *de factor* hinge zones due to the present 4-neighborhood connectivity measure rather than the node-connection measure [Han, Xu, and Prince (2003)]. In the work of [Chen, Wang, Wang, and Xia (2005); Wang, Chen, Wang, and Mei (2005)], since only some preliminary analysis based on image processing was introduced, the structural connectivity and the topology optimization could not be guaranteed simultaneously. Since the structural connectivity can be preserved at the discrete 0-1 level during the level set evolution, the present method can be significantly different from the conventional level set methods [Osher and Santosa (2001); Wang, Wang, and Guo (2003); Allaire, Jouve, and Toader (2004)], in which the occurrence of *de factor* hinge zones cannot be prevented, as shown in [Wang, Chen, Wang, and Mei (2005)]. In the field of shape and topology optimization, the popular continuum optimal topology design using the homogenization-based methods [Bendsøe and

Sigmund (2003)] cannot eliminate the occurrence of the *de facto* hinge zones either, which are generally regarded as improper designs [Rahmatalla and Swan (2005)], depending on the the objective functions and the artificial spring models used. It should also be noted that the region identification technique introduced in this study is not time consuming in general since the FE-based structural analysis in shape and topology optimization usually dominates the computational time.

Figure 5 illustrates the present structural connectivity preserving analysis during the level set evolution. The structurally connected binary image  $\mathfrak{S}_t$  at time  $t$ , as shown in Fig. 5(b), is obtained from the design at time  $t$ , as shown in Fig. 5(a). It becomes a structurally disconnected binary image  $\mathfrak{S}_{\text{exp}}$  after an exploratory move, as shown in Fig. 5(c). The removed solid elements  $C_{\text{rem}}$  during the exploratory move can be found and labelled as removed components  $C_{\text{rem}}^{\text{lab}}$ , as shown in Fig. 5(d). Further analysis on the components  $C_{\text{rem}}^{\text{lab}}$  removed from  $\mathfrak{S}_t$ , as shown in Fig. 5(b), can identify the crucial components  $C_c^{\text{lab}}$  which are necessary to preserve the structural connectivity of  $\mathfrak{S}_t$ , as shown in Fig. 5(e). Those crucial components are recovered in the resulting binary image  $\tilde{\mathfrak{S}}_{\text{exp}}$  to satisfy the structural connectivity requirements during the level set evolution, as shown in Fig. 5(f). Hence, the structural connectivity can be well preserved after an actual move at time  $t$ .

### 2.3 A Structural Connectivity and Topology Preserving Level Set Method

The present structural connectivity preserving level set method can be further developed into a structural connectivity and topology preserving level set method such that the mere boundary-based structural shape optimization in addition to simultaneous shape and topology optimization can be performed using the level set methods. Similar to the structural connectivity preserving analysis, the structural connectivity and topology preserving analysis needs to identify crucial components  $C_c^{\text{lab}}$  from the the removed components  $C_{\text{rem}}^{\text{lab}}$  during an exploratory move which are necessary to maintain the structural connectivity as well as preserve the topology. Besides the struc-

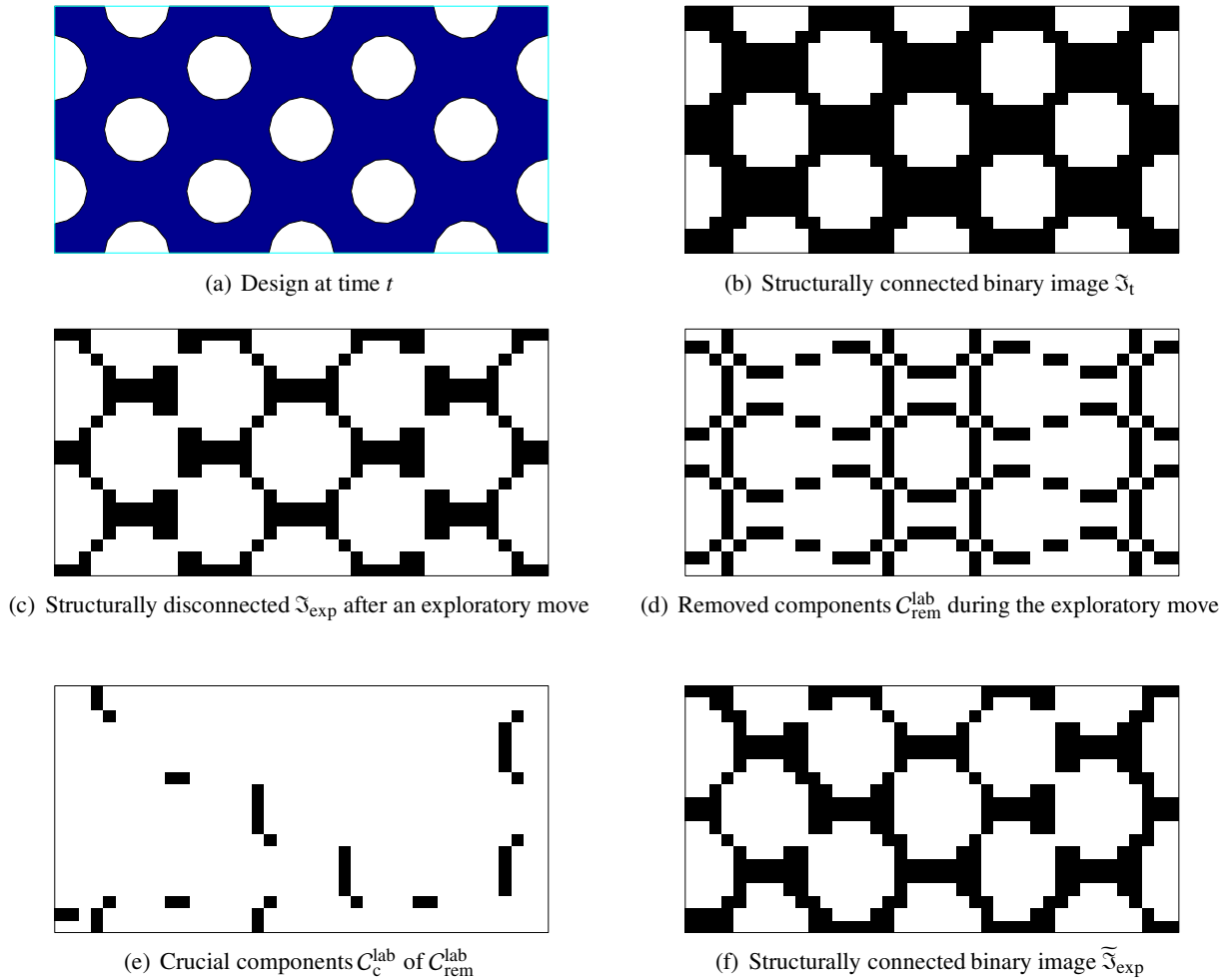


Figure 5: Structural connectivity preserving analysis during the level set evolution.

tural connectivity condition, a removed component will also be identified as a crucial component if its removal from the binary image  $\mathfrak{S}_t$  may cause a topological change measured by the total number of internal holes in this study. This handling to prevent the topological changes can be justified since there is no nucleation mechanism in the conventional level set methods [Osher and Fedkiw (2002); Burger, Hackl, and Ring (2004); Amstutz and Andr a (2006)] and thus the topological changes are only due to the elimination of the internal holes. Hence, the recovery of the removed components crucial to structural connectivity and topology will lead to a structural connectivity and topology preserving design during the level set evolution.

Figure 6 demonstrates the present structural connectivity and topology preserving analysis. The structurally connected binary image  $\mathfrak{S}_t$  with 6 internal holes at time  $t$  becomes structurally disconnected with topological changes after an exploratory move since one-node connection is considered as disconnected by the present 4-neighborhood connectivity measure, as shown in Fig. 6(c). After a region identification of both Figs. 6(b) and 6(c), the removed components  $C_{rem}^{lab}$  during the exploratory move can be obtained and labelled, as shown in Fig. 6(d). Further analysis on the components  $C_{rem}^{lab}$  removed from  $\mathfrak{S}_t$  can find  $C_c^{lab}$  crucial to preserve the structural connectivity and topology, as shown in Fig. 6(e). Those necessary components are recovered in the final

binary image  $\widetilde{\mathfrak{T}}_{\text{exp}}$ , as shown in Fig. 6(f). Hence, the structural connectivity and topology at the discrete 0-1 level can both be preserved after a move at time  $t$ .

### 3 An Implementation of Structural Shape and Topology Optimization Using the Level Set Methods

#### 3.1 Shape and Topology Optimization Using the Level Set Methods

Using a level set model as defined in Eq. (1), the usual structural shape and topology optimization problem with a volume constraint [Sigmund (2001); Bendsøe and Sigmund (2003)] to limit the use of material can be written as follows:

$$\begin{aligned} \min_{\Phi} \quad & J(\mathbf{u}, \Phi) = \int_{\mathcal{D}} F(\mathbf{u})H(-\Phi)d\Omega \\ \text{s.t.} \quad & a(\mathbf{u}, \mathbf{v}, \Phi) = L(\mathbf{v}, \Phi), \quad \mathbf{u}|_{\Gamma_D} = \mathbf{u}_0, \quad \forall \mathbf{v} \in \mathcal{U} \\ & V(\Phi)/V_0 = \zeta \end{aligned} \quad (10)$$

where  $J(\mathbf{u}, \Phi)$  is the objective function,  $\mathbf{u}$  the displacement field,  $F(\mathbf{u})$  the design function,  $H(\Phi)$  the Heaviside step function,  $V(\Phi)$  the material volume,  $V_0$  the total volume of the design domain  $\mathcal{D}$ , and  $\zeta$  the prescribed volume fraction. The linearly elastic equilibrium equation is written in its weak variational form in terms of the energy bilinear form  $a(\mathbf{u}, \mathbf{v}, \Phi)$  and the load linear form  $L(\mathbf{v}, \Phi)$  [Wang and Wang (2004b)], with  $\mathbf{v}$  denoting a virtual displacement field in the space  $\mathcal{U}$  of kinematically admissible displacement fields, and  $\mathbf{u}_0$  the prescribed displacement on the admissible Dirichlet boundary  $\Gamma_D$ . Furthermore, we have

$$a(\mathbf{u}, \mathbf{v}, \Phi) = \int_{\mathcal{D}} \boldsymbol{\varepsilon}^T(\mathbf{u})\mathbf{C}\boldsymbol{\varepsilon}(\mathbf{v})H(-\Phi)d\Omega \quad (11)$$

$$\begin{aligned} L(\mathbf{v}, \Phi) = \int_{\mathcal{D}} \mathbf{v}^T \mathbf{f} H(-\Phi) d\Omega \\ + \int_{\mathcal{D}} \mathbf{v}^T \boldsymbol{\tau} \delta(\Phi) |\nabla \Phi| d\Omega \end{aligned} \quad (12)$$

$$V(\Phi) = \int_{\mathcal{D}} H(-\Phi) d\Omega \quad (13)$$

where  $\mathbf{C}$  is the elasticity matrix,  $\mathbf{f}$  the body force vector,  $\boldsymbol{\tau}$  the boundary traction force vector, and  $\delta(\Phi)$  the Dirac delta function.

In the present geometric deformation constrained level set method, since both the structural connectivity and topology may be preserved, simultaneous shape and topology optimization as well as mere shape optimization can be performed by solving (10). The Lagrange multiplier method can be used to solve this optimization problem [Osher and Santosa (2001)]. By setting the constraint on the equilibrium state inactive, the Lagrangian  $\mathcal{L}(\mathbf{u}, \Phi, \ell)$  with a positive Lagrange multiplier  $\ell$  can be given by

$$\mathcal{L}(\mathbf{u}, \Phi, \ell) = J(\mathbf{u}, \Phi) + \ell G(\Phi) \quad (14)$$

where the volume constraint functional  $G(\Phi)$  can be expressed as

$$G(\Phi) = V(\Phi) - \zeta V_0 \quad (15)$$

According to the Kuhn-Tucker condition of the optimization, the necessary condition for a minimizer is

$$\begin{aligned} D_{\Phi} \mathcal{L}(\mathbf{u}, \Phi, \ell) = 0 \\ G(\Phi) = 0 \end{aligned} \quad (16)$$

where  $D_{\Phi} \mathcal{L}(\mathbf{u}, \Phi, \ell)$  is the gradient of the Lagrangian with respect to  $\Phi$ . It should be noted that  $\mathbf{u}$  is also a function of  $\Phi$ , i.e.  $\mathbf{u} = \mathbf{u}(\Phi)$ .

#### 3.2 Normal Velocities

The gradient, or shape derivative, of the Lagrangian  $D_{\Phi} \mathcal{L}(\Phi, \ell)$  may be obtained following the well-known approach of Murat and Simon of shape diffeomorphism [Haug, Choi, and Komkov (1986); Sokolowski and Zolesio (1992)]. Based on local perturbations of the moving free boundary of an admissible design [Wang and Wang (2004b)], the resulting shape derivative of the Lagrangian can be written as

$$\begin{aligned} D_{\Phi} \mathcal{L}(\mathbf{u}, \Phi, \ell) \\ = \int_{\mathcal{D}} (g(\mathbf{u}, \Phi) + \ell) \delta(\Phi) |\nabla \Phi| v_n d\Omega \end{aligned} \quad (17)$$

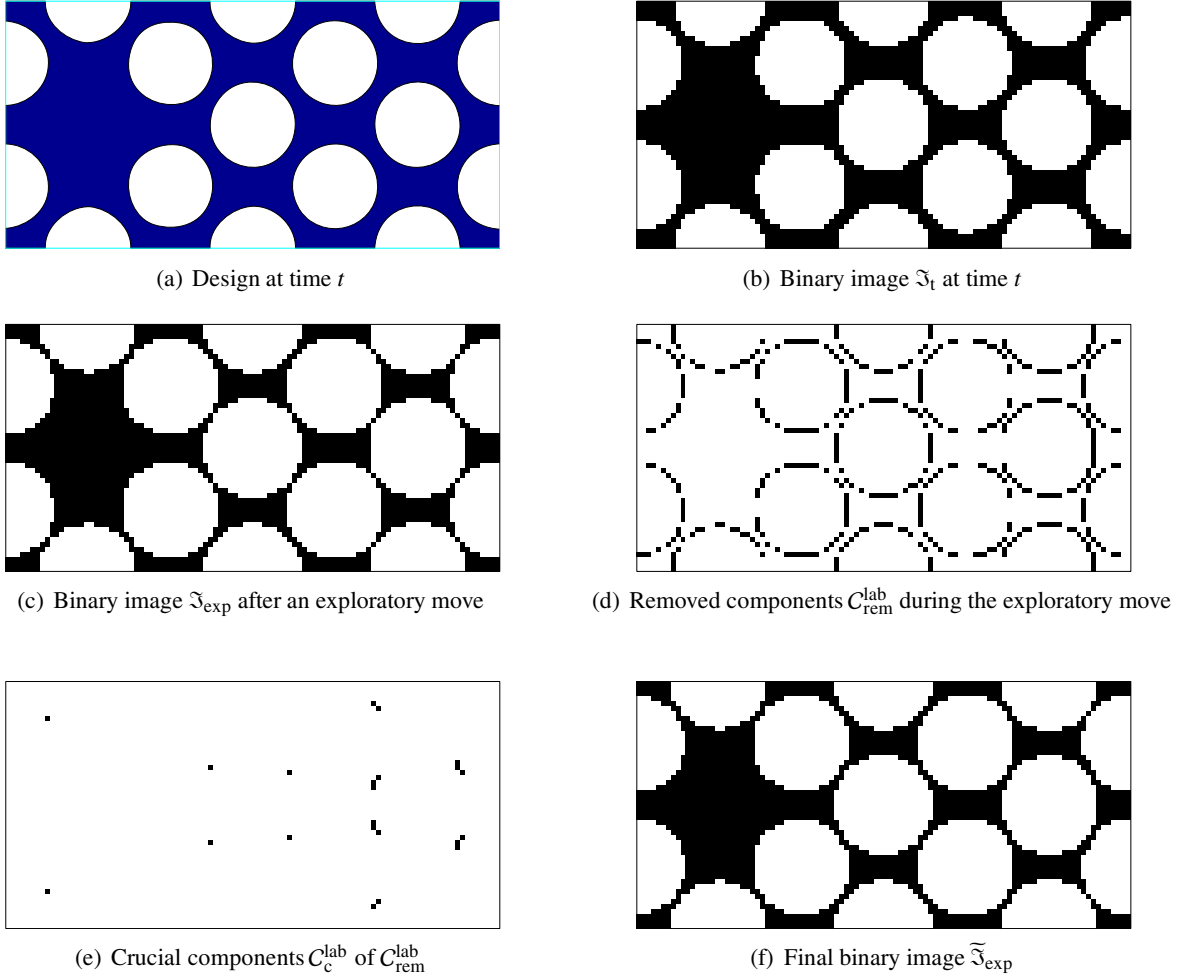


Figure 6: Structural connectivity and topology preserving analysis during the level set evolution.

where

$$g(\mathbf{u}, \Phi) = F(\mathbf{u}) + (\mathbf{u}^*)^T (\mathbf{f} + \kappa \boldsymbol{\tau}) + \nabla((\mathbf{u}^*)^T \boldsymbol{\tau}) \cdot \mathbf{n} - \boldsymbol{\varepsilon}^T(\mathbf{u}) \mathbf{C} \boldsymbol{\varepsilon}(\mathbf{u}^*) \quad (18)$$

in which  $\mathbf{u}^*$  is the adjoint displacement field of  $\mathbf{u}$ , and the curvature  $\kappa$  can be given as

$$\kappa = \nabla \cdot (\nabla \Phi / |\nabla \Phi|) \quad (19)$$

Furthermore, Eq. (17) can be simplified as

$$D_{\Phi} \mathcal{L}(\mathbf{u}, \Phi, \ell) = \int_{\Gamma_M} (g(\mathbf{u}, \Phi) + \ell) v_n ds \quad (20)$$

where  $\Gamma_M$  is the moving free boundary. Similarly, the resulting shape derivative of the volume

constraint functional  $G(\Phi)$  (15) can be simply expressed as

$$D_{\Phi} G(\Phi) = \int_{\Gamma_M} v_n ds \quad (21)$$

In the present shape and topology optimization using the level set methods, choosing the normal velocity field  $v_n$  is equivalent to choosing a descent direction for the Lagrangian  $\mathcal{L}(\mathbf{u}, \Phi, \ell)$ , which can be readily implemented by using the steepest gradient method extensively employed in the literature [Osher and Santosa (2001); Wang, Wang, and Guo (2003); Allaire, Jouve, and Toader (2004); Wang and Wang (2006a,c)]. According to the shape derivative of the Lagrangian in Eq. (20), a descent direction of the normal velocity  $v_n$  for the Lagrangian can be obtained by

simply identifying the normal velocity  $v_n$  as

$$v_n = -g(\mathbf{u}, \Phi) - \ell \quad (22)$$

in which the adjoint displacement field  $\mathbf{u}^*$  may be involved, as shown in (18). For the present problem with a moving free boundary, without remeshing, the displacement fields may be accurately and efficiently obtained by using several existing numerical methods such as the "ersatz material" approach [Allaire, Jouve, and Toader (2004)], the geometry projection method [Norato, Haber, Tortorelli, and Bendsøe (2004)], the extended finite element methods [Belytschko and Black (1999); Strouboulis, Copps, and Babuska (2001); Belytschko, Xiao, and Parimi (2003); Wang and Wang (2006a)], or the true meshless local Petrov-Galerkin method [Atluri and Shen (2002)]. In the present study, only the relatively simple "ersatz material" approach is adopted, which is well-known in topology optimization and can be rigorously justified in some cases [Allaire (2001); Allaire, Jouve, and Toader (2004); Wang and Wang (2006a)]. In numerical practice of the "ersatz material" approach, material density is assumed to be piecewise constant in each element and is adequately interpolated in those elements cut by the moving free boundary  $\Gamma_M$ .

It should be stressed that the present normal velocity field  $v_n$  can guarantee that the final design be monolithic, though polyolithic designs may appear during the level set evolution. In the present geometric deformation constrained level set method, there is only one structurally connected component in a polyolithic design. The structurally disconnected components, which cannot connect the input ports and the output ports properly through structural deformation, do not possess the mechanical strains. Hence, we have

$$\boldsymbol{\varepsilon}(\mathbf{u}) = \boldsymbol{\varepsilon}(\mathbf{u}^*) = 0 \quad (23)$$

Due to the lack of mutual strain energy, it can be derived that if the design function  $F(\mathbf{u})$  is energy-based, the normal velocity at the free boundary of those components is:

$$v_n = -\ell \quad (24)$$

This negative velocity field will drive the free boundary to move inwardly during the level set evolution and thus the volumes of the structurally disconnected components may become smaller and smaller. At the convergence, those components may disappear and a monolithic design may be finally reached.

### 3.3 Extension Velocities

The normal velocity  $v_n$  defined at the moving free boundary  $\Gamma_M$  must be extended in the Eulerian capturing level set methods, either to the whole design domain  $\mathcal{D}$  [Allaire, Jouve, and Toader (2004)] or to a narrowband around the free boundary [Osher and Fedkiw (2002)]. The choice of an extension velocity method is crucial since it can directly influence the overall efficiency of the level set methods [Sethian (1999)].

In this study, a physically meaningful extension velocity method without the additional PDE solving procedure is presented. According to Eq. (22), a natural extension of the normal velocity  $v_n$  at the free boundary can be obtained if the displacement field  $\mathbf{u}$  is extended to the entire design domain  $\mathcal{D}$  by assuming that  $\mathbf{u} = 0, \mathbf{u} \in (D \setminus \Omega)$ . This natural extension velocity method is simple and easy to implement and the conventional PDE solving procedure in extending the normal velocities at the free boundary [Sethian (1999)] is not needed. Nevertheless, direct use of these natural extension velocities may cause numerical instabilities, which are well known in the field of shape and topology optimization due to the ill-posedness of the optimization problem [Bendsøe and Sigmund (2003); Allaire, Jouve, and Toader (2004); Wang and Wang (2006a)]. To regularize the ill-posed problem into a well-posed problem, a filtering technique, which has become quite popular and successful in various domains of applications as a numerical method to ensure regularity or existence of solutions to an ill-posed engineering problem and has become a major regularization method in the continuum topology optimization [Bendsøe and Sigmund (2003); Wang and Wang (2005a)], is employed to smooth the natural extension velocities. It should be noted that a perimeter control method has been presented

to smooth the extension velocities in the literature [Allaire, Jouve, and Toader (2004); Wang and Wang (2004a)].

In the present implementation, a linear smoothing filter is introduced for the extension velocities in a narrowband region around the moving free boundary to achieve the computational efficiency. The extension velocity  $v_n^e$  in the narrowband is smoothed as  $\widehat{v}_n^e$  by using a linear hat kernel function [Sigmund (2001)] to achieve an excellent edge smoothing effect [Wang and Wang (2005a)], which can be written as

$$\widehat{v}_n^e = \widehat{v}_n^e(\mathbf{x}) = k^{-1}(\mathbf{x}) \sum_{\mathbf{p} \in N(\mathbf{x})} w(\|\mathbf{p} - \mathbf{x}\|) v_n^e(\mathbf{x}) \quad (25)$$

where

$$w(\|\mathbf{p} - \mathbf{x}\|) = r_{\min} - \|\mathbf{p} - \mathbf{x}\| \quad (26)$$

$$k(\mathbf{x}) = \sum_{\mathbf{p} \in N(\mathbf{x})} w(\|\mathbf{p} - \mathbf{x}\|) \quad (27)$$

in which  $N(\mathbf{x})$  is the neighborhood of  $\mathbf{x}$  in the 2D filter window and  $r_{\min}$  the filter window size.

### 3.4 Lagrange Multiplier

The Lagrange multiplier  $\ell$  in (22) can be obtained by solving the volume constraint equation  $G(\Phi) = 0$  in (16), which will greatly restrict the geometric deformation of a level set model. Since the variation of the total volume  $V(\Phi)$  is due to the extension velocities in the capturing level set methods, we have

$$V(\Phi) = V(v_n) = V(v_n^e) = V(\ell) \quad (28)$$

Furthermore, it can be found that  $V(\ell)$  is a monotonically decreasing function of  $\ell$  since a smaller  $\ell$  will cause the velocity  $v_n$  as well as the volume  $V(\Phi)$  to become larger due to the more outward movement along the normal direction, according to (22). This monotonicity makes the fast convergent bi-sectioning algorithm [Sigmund (2001); Wang and Wang (2006c)] suitable and efficient for solving the constraint equation in (16), which can be re-written as

$$G(\Phi) = V(\ell) - \zeta V_0 = 0 \quad (29)$$

The bi-sectioning algorithm is initialized by setting a lower bound  $\ell_1$  and an upper bound  $\ell_2$  for the Lagrange multiplier  $\ell$ . The interval which bounds the Lagrange multiplier is halved and the Lagrange multiplier is given by  $\ell = (\ell_1 + \ell_2)/2$ . Based on the sign of the error in solving Eq. (29) using this Lagrange multiplier, either the lower bound  $\ell_1$  or the upper bound  $\ell_2$  can be updated. The interval which bounds the Lagrange multiplier can be repeatedly halved until its size is less than the convergence criteria.

By using this relatively simple algorithm, the complexities in boundary integration of the mutual energy density [Wang, Wang, and Guo (2003)] can be circumvented and the additional efforts to put the iteration back to the feasible set to eliminate the significant volume fluctuations [Osher and Santosa (2001)] would become redundant. The present implementation can thus be both accurate and efficient. Since the total volume constraint may be satisfied accurately to make full use of the given material, the present geometric deformation constrained level set method can be not only structural connectivity and/or topology preserving to guarantee properly connected designs, but also volume conservative to generate feasible designs during the course of evolution.

## 4 Numerical Examples and Discussion

Numerical examples are provided to illustrate the effectiveness of the present geometric deformation constrained level set method for structural shape and topology optimization. Unless stated otherwise, all the units are consistent and the following parameters are assumed as: the Young's elasticity modulus  $E = 1$  for solid materials,  $E = 1 \times 10^{-5}$  for void materials, and Poisson's ratio  $\nu = 0.3$ . For all examples, a fixed rectilinear FE mesh is specified over the entire design domain  $\mathcal{D}$  for the structural analysis of the designs. The present numerical calculation will be terminated when the relative difference between two successive objective function values is less than  $10^{-5}$  or when the given maximum number of iterations has been reached.

#### 4.1 Shape and/or Topology Optimization of a Cantilever

The minimum compliance design problem of shape and topology optimization of a short cantilever, as shown in Fig. 7, is considered. The whole design domain  $\mathcal{D}$  is a rectangle of size  $2 \times 1$  with a fixed boundary  $\partial D$  on the left side and a unit vertical point load  $P = 1$  applied at a fixed non-homogeneous Neumann boundary  $\partial D_N$ , the middle point of the right side. The prespecified material volume fraction is  $\zeta = 0.5$ . A regular mesh of  $80 \times 40$  is used in the spatial discretization. The present geometric deformation constrained level set method is used to perform simultaneous shape and topology optimization as well as mere shape optimization of this cantilever.

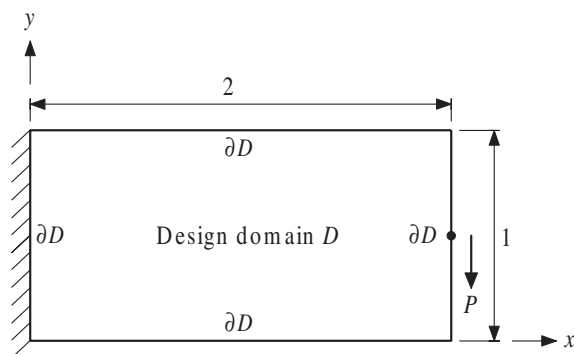


Figure 7: Minimum compliance design problem of a cantilever beam.

Figure 8 displays the evolution history of an optimal design for simultaneous shape and topology optimization of the cantilever using the present structural connectivity preserving level set method. It can be seen that the structural connectivity can be well maintained during the level set evolution. As expected, a monolithic final design may be approximately achieved at the convergence of the objective function. It should be noted that for this minimum compliance optimization problem the structural connectivity can be preserved without the additional explicit structural connectivity constraint due to the stiffest design objective and the relatively small timestep size constricted by the CFL condition [Sethian (1999);

Osher and Fedkiw (2002)]. The convergence of the objective and volume functions is shown in Fig. 9. The objective function converges smoothly due to the present filtered extension velocities. The volume constraint can be almost exactly satisfied during the iterations due to the present bisectioning algorithm. Hence, the present volume constraint handling approach is effective to keep the total volume conservative.

The distinctive features of the present geometric deformation constrained level set method are further illustrated by performing boundary-based shape optimization of the cantilever with different topologies. Figure 10 shows the evolution history of a final design for shape optimization of the cantilever with 6 internal holes. The topology of the initial design shown in Fig. 10(a) is in fact the same as that of the final design shown in Fig. 8(f) for simultaneous shape and topology optimization of the cantilever since the number of internal holes is the same. It can be seen that by using the present geometric deformation constrained level set method both the structural connectivity and topology can be well preserved during the level set evolution. The effectiveness of the present geometric deformation constrained level set method is thus demonstrated. The accuracy of the present shape optimization may be verified by the excellent agreement between the boundary of the final design shown in Fig. 8(f) and the zero normal velocity curve shown in Fig. 11. Theoretically, the final design possesses zero normal velocities at its free boundary such that a homogeneous stress distribution along the free boundary may be arrived at, as discussed in detail in [Wang and Wang (2006c)]. Again, it can be seen from Fig. 10 that the final design is monolithic. The convergence of the objective and volume functions is shown in Fig. 11. The objective function converges smoothly due to the fact that the present constraint on the geometric deformation does not change the decrease of the objective function because of the steepest gradient method, as aforementioned. The convergence speed of shape optimization is quite slow since the boundary-based shape optimization is usually time consuming, as detailed in [Bendsøe and Sig-

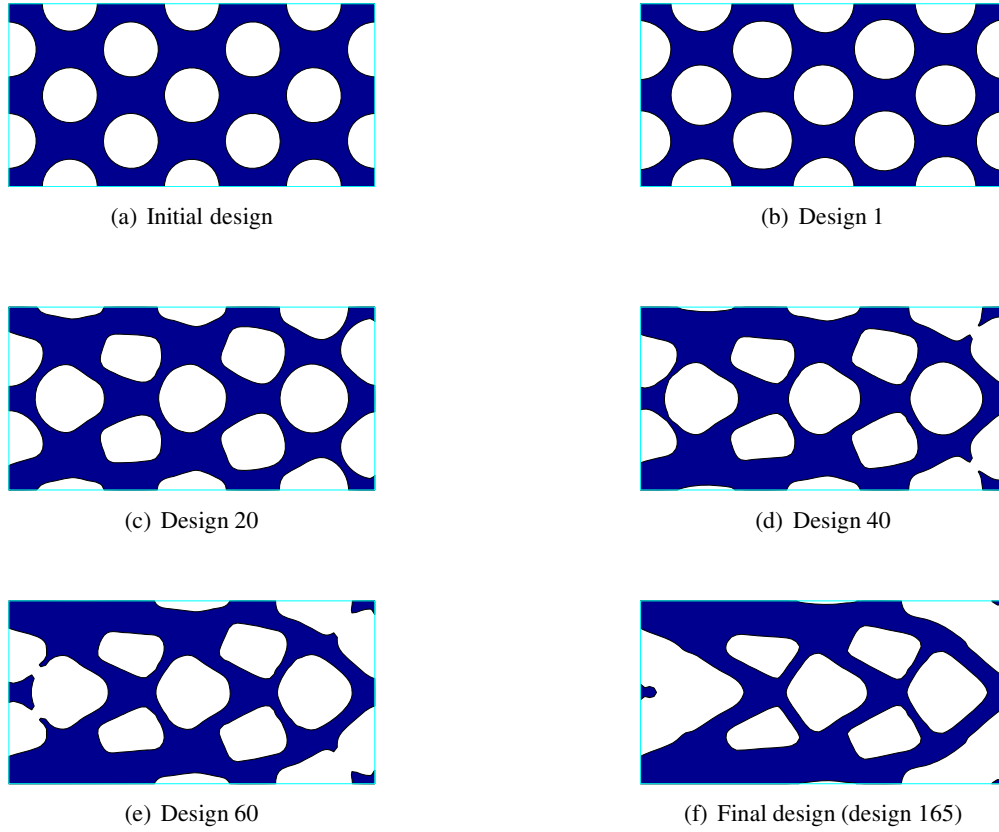


Figure 8: Evolution history of an optimal design for simultaneous shape and topology optimization.

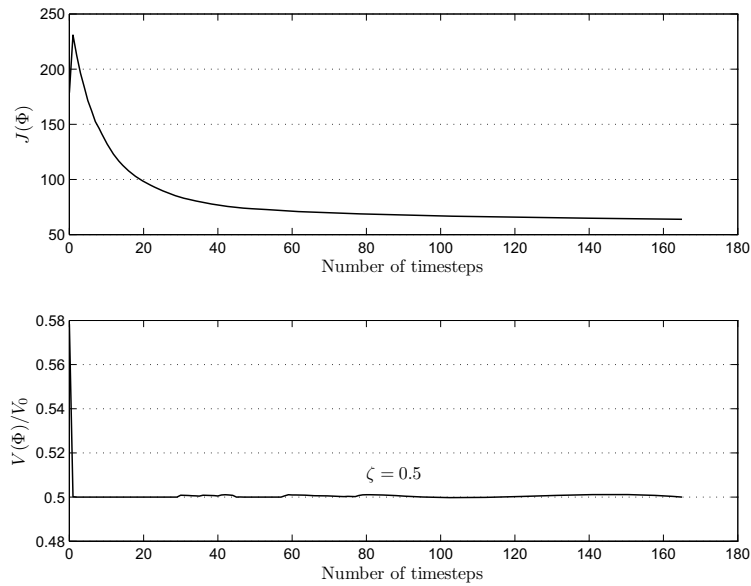


Figure 9: Convergence of objective and volume functions for the cantilever.

mund (2003)]. It should be noted that the conventional level set methods [Wang, Wang, and Guo (2003); Allaire, Jouve, and Toader (2004); Wang and Wang (2004a)] cannot preserve the topology during the course of evolution due to the lack of a geometric deformation constraint. The effectiveness of the present method in boundary-based shape optimization is further illustrated in Fig. 13, in which the topology is with 7 internal holes. During the level set evolution, the strong tendency to change the topology to further improve the objective function is successfully prevented due to the fact that the present level set method is topology preserving at the discrete 0-1 level. Again, Fig. 14 shows that the objective function can be smoothly convergent and the total volume can be conservative. Figure 15 displays the evolution history of a final design for the boundary-based shape optimization of the cantilever with 3 internal holes. It can be seen that topological changes are actually prohibited due to the present topology preserving level set method and the final design is quite smooth due to the present extension velocities. The present method may guarantee the smooth convergence of the objective function while generating feasible designs during the evolution, as shown in Fig. 16. It should be noted that the topology shown in Fig. 15 is also the optimal topology predicted for this problem by a popular homogenization-based continuum topology optimization method (the power-law approach) [Sigmund (2001)]. Since the element relaxing-based method in [Sigmund (2001)] is less accurate than the present moving boundary-based level set method in general, it can be expected that the resulting optimal topology could be less effective. In fact, after the present boundary-based shape optimization, the objective function value (61.84) of the final design shown in Fig. 15(f) is worse than that (60.76) of the final design shown in Fig. 10(f), which may suggest that the corresponding topology could be less effective than the one predicted by the present simultaneous shape and topology optimization, as shown in Fig. 8.

#### 4.2 Topology Optimization of an Inverter Mechanism

The present level set method is further applied to topology optimization of compliant mechanisms, which has been investigated by many other researchers using different methods [Yin and Ananthasuresh (2003); Bendsøe and Sigmund (2003); Rahmatalla and Swan (2005); Wang, Chen, Wang, and Mei (2005)]. An inverter mechanism [Bendsøe and Sigmund (2003)], as shown in Fig. 17, is first adopted. In Fig. 17(b), the workpiece is modeled by an artificial spring with a stiffness  $k_{out}$  under the action of an input actuator modeled by another artificial spring with a stiffness  $k_{in}$  and a force  $f_{in}$  and a displacement  $u_{in}$ . The  $1 \times 1$  square design domain  $\mathcal{D}$  is discretized by a regular FE mesh of  $100 \times 100$ . Due to the symmetry, only a half structure is used in the analysis to reduce the computational cost. It is assumed that  $k_{in} = k_{out}$ ,  $f_{in} = 2$ , and a volume fraction of  $\zeta = 0.3$ .

Figure 18 shows the optimal design for the inverter mechanism using a conventional level set method without the present explicit geometric deformation constraint. Due to the lack of a geometric deformation constraint and the relatively low stiffness of the artificial springs ( $k_{in} = k_{out} = 0.008$ ), the final design is structurally disconnected. Hence, a conventional level set method cannot guarantee the structural connectivity of a design. Similar results can be observed in [Wang, Chen, Wang, and Mei (2005)], in which structurally disconnected designs are generated during the level set evolution. The structural disconnectedness of a final design should be avoided since the design would become structurally unusable and the corresponding artificial material-based FE analysis [Allaire, Jouve, and Toader (2004)], as shown in Fig. 20(a), would become questionable due to the inaccuracy of the use of a weak material to eliminate the singularity. In the popular element-based continuum topology optimization methods [Bendsøe and Sigmund (2003)], this phenomenon is indicated by the occurrence of *de factor* hinge zones. Although many efforts have been made [Yin and Ananthasuresh (2003); Bendsøe and Sigmund (2003); Rahmatalla and Swan (2005); Wang, Chen, Wang, and Mei (2005)] to

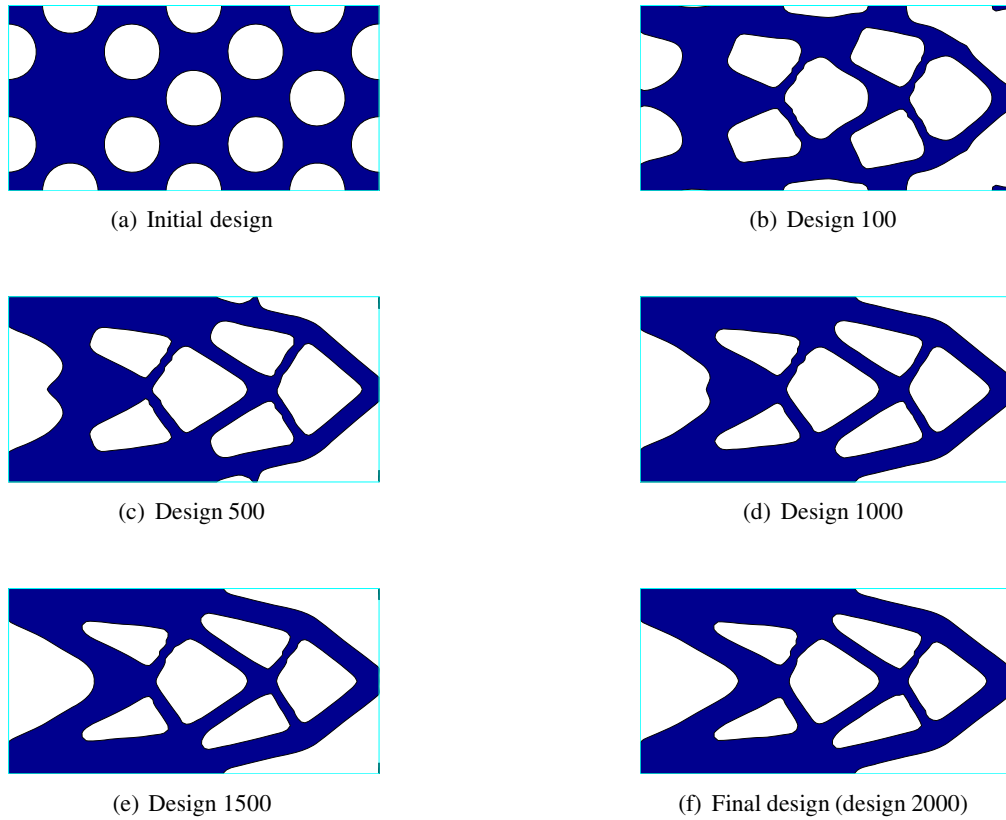


Figure 10: Evolution history of a final design for shape optimization of the cantilever with 6 holes.

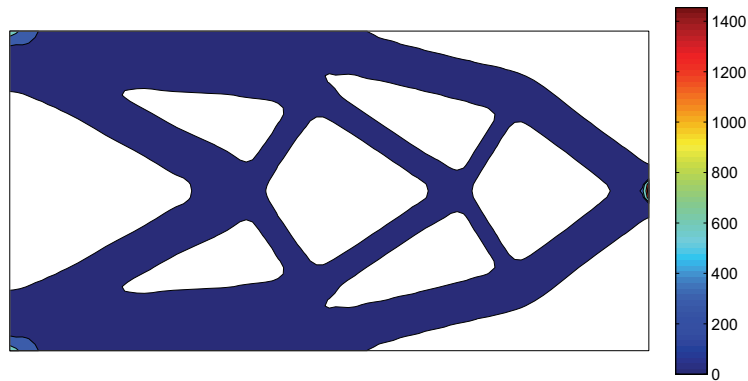


Figure 11: Scalar velocity field ( $v_n^e \geq 0$ ) of the final design for shape optimization of the cantilever.

eliminate this phenomenon to guarantee reliable designs, only limited success was reported since a geometric deformation constraint was not properly introduced.

Figure 19 displays the evolution history of a final design for the inverter mechanism using the

present geometric deformation constrained level set method ( $k_{in} = k_{out} = 0.008$ ). During the evolution, the structural connectivity can be well maintained since the present moving boundary-based method can be structural connectivity preserving at a discrete 0-1 level. The final design is thus structurally connected and can even be mono-

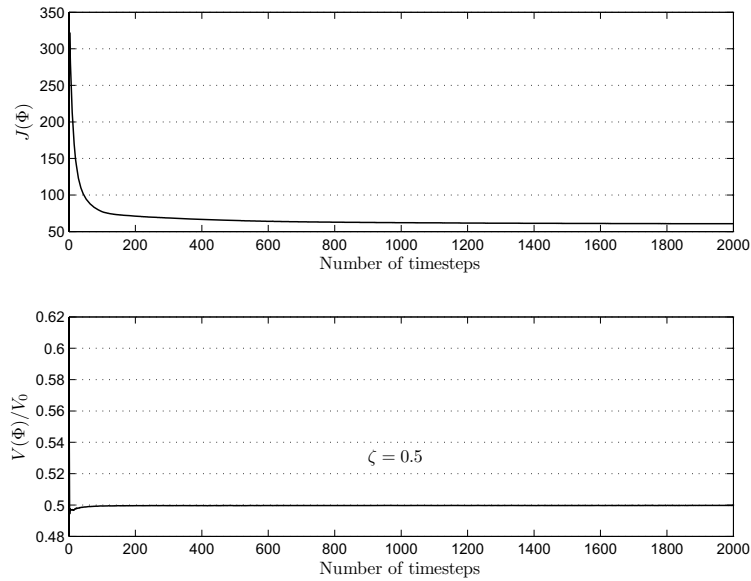


Figure 12: Convergence of objective and volume functions for shape optimization of the cantilever with 6 holes.

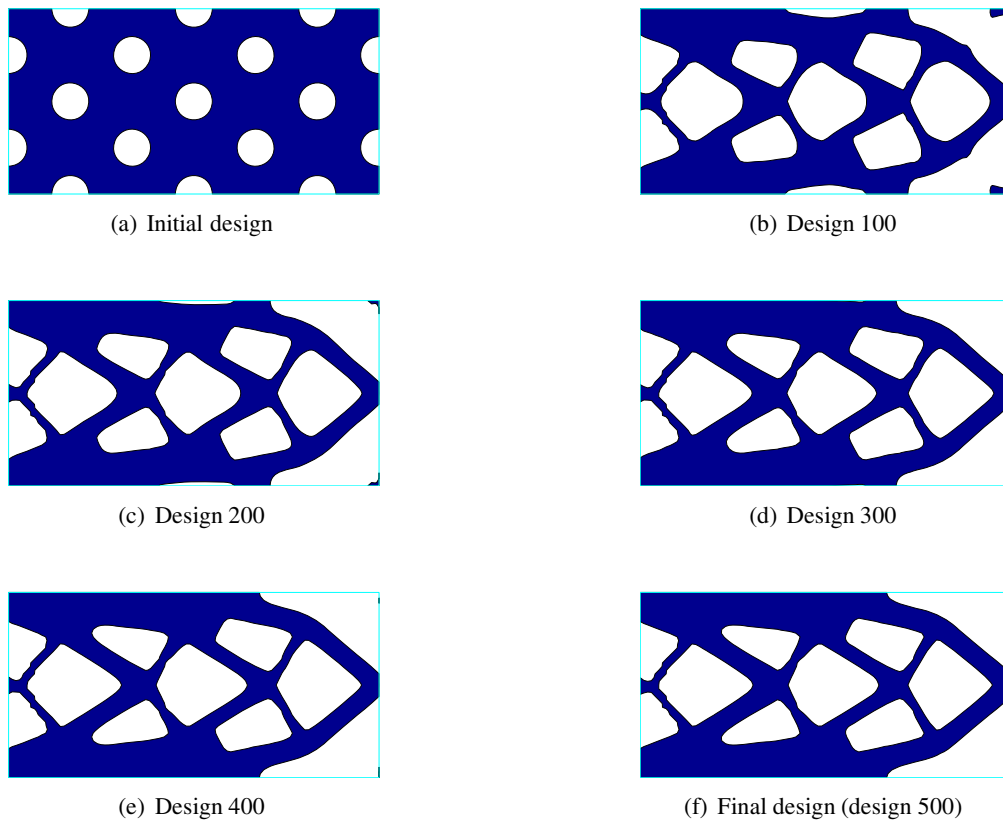


Figure 13: Evolution history of a final design of shape optimization of the cantilever with 7 holes.

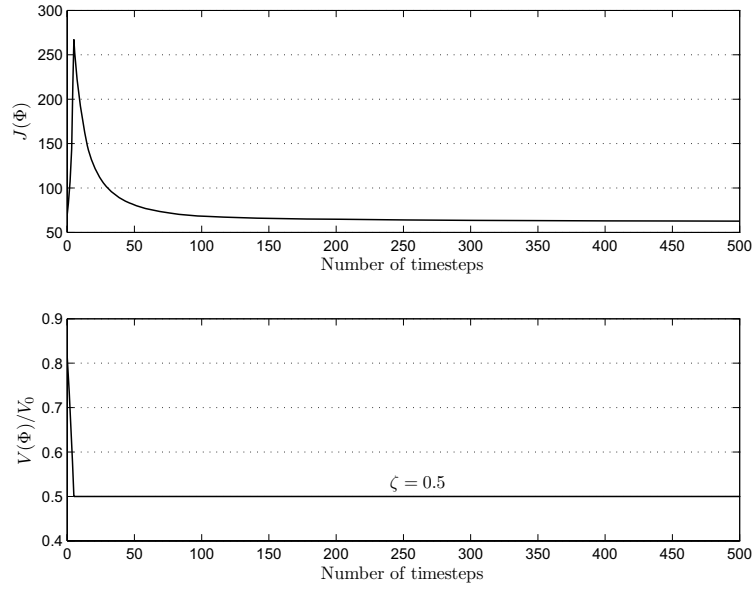


Figure 14: Convergence of objective and volume functions for shape optimization of the cantilever with 7 holes.

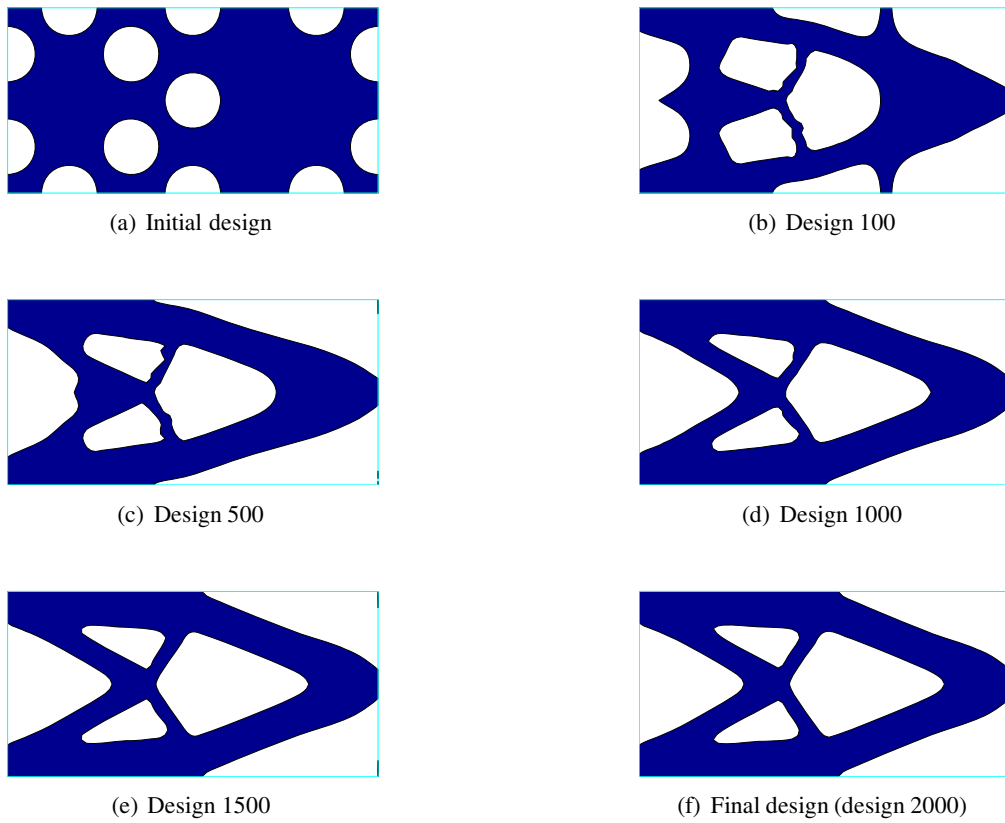


Figure 15: Evolution history of a final design for shape optimization of the cantilever with 3 holes.

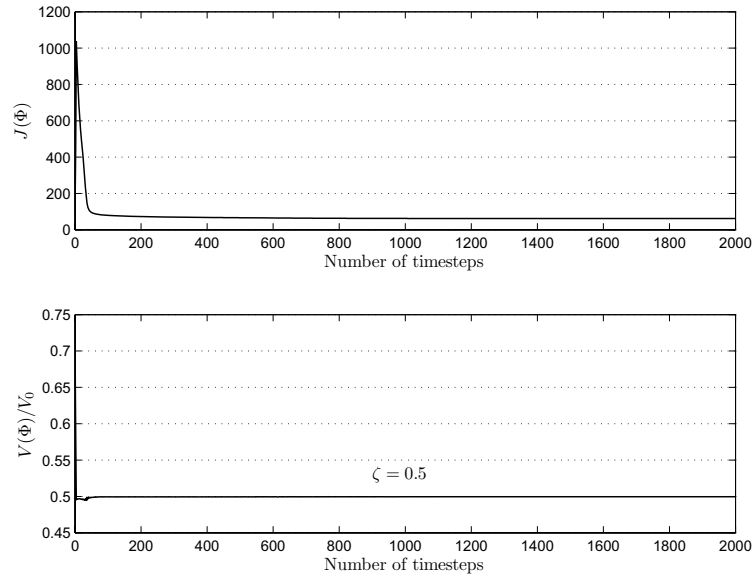


Figure 16: Convergence of objective and volume functions for shape optimization of the cantilever with 3 holes.

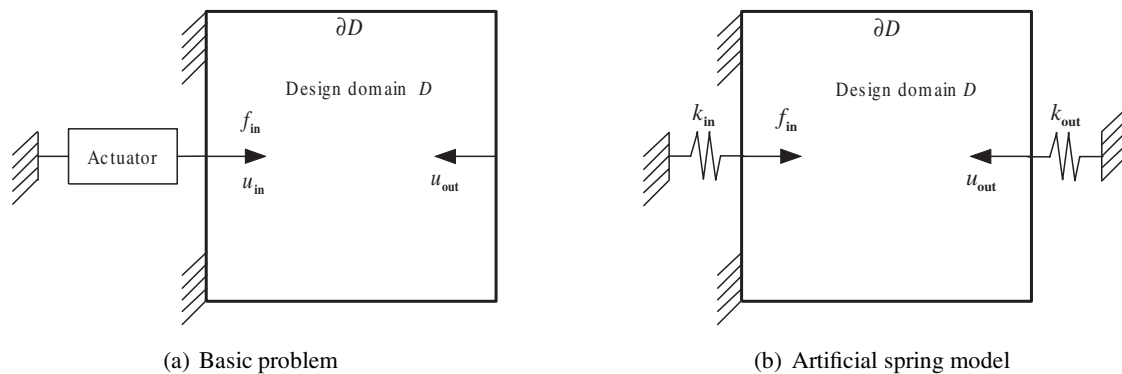


Figure 17: Inverter mechanism design problem.

lithic, as aforementioned. The corresponding FE model, as shown in Fig. 20(b), can be consistent with the final design and the inaccurate FE model featuring *de factor* hinges popular in continuum topology optimization of compliant mechanisms [Bendsøe and Sigmund (2003)], as shown in Fig. 20(a), is avoided. The development of structurally disconnected design is successfully prevented. The effectiveness of the present structural connectivity preserving level set method is thus further demonstrated. The resulting design shown in Fig. 19 can be different from the one shown in Fig. 18 using a conventional level set

method due to the present explicit geometric deformation constraint. It should also be noted that the present method is independent of the artificial spring model widely adopted in compliant mechanism design [Bendsøe and Sigmund (2003)]. Hence, the present method can be of a significant improvement over the existing level set methods [Wang, Wang, and Guo (2003); Wang, Chen, Wang, and Mei (2005); Allaire, Jouve, and Toader (2004)] in achieving reliable and properly connected designs.

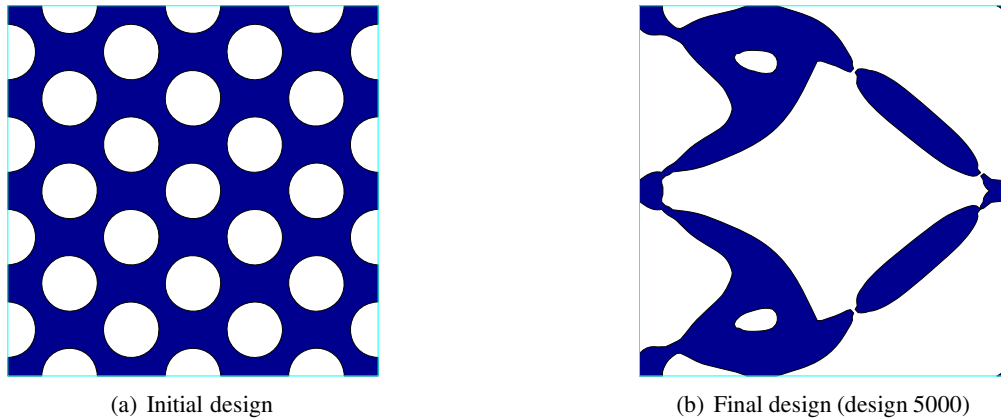


Figure 18: Optimal design for the inverter mechanism using a conventional level set method ( $k_{\text{in}} = k_{\text{out}} = 0.008$ ).

### 4.3 Topology Optimization of a Gripper Mechanism

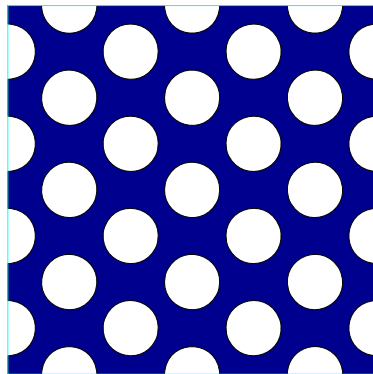
A gripper mechanism [Rahmatalla and Swan (2005)], as shown in Fig. 21, is employed. The  $1 \times 1$  design domain  $\mathcal{D}$  is discretized by a mesh of  $100 \times 100$ . Only a half structure is used in the analysis of this symmetric problem to save the computational time. It is assumed that  $k_{\text{in}} = k_{\text{out}}$ ,  $f_{\text{in}} = 2$ , and a volume fraction of  $\zeta = 0.3$ .

Figure 22 displays an optimal design for the gripper mechanism using a conventional level set method. Again, the final design is structurally disconnected since the conventional level set method may destroy the structural connectivity of a design during the level set evolution. Figure 23 shows the evolution history of an optimal design using the present level set method. It can be seen that the structural connectivity can be well maintained during the course of evolution due to the distinct structural connectivity preserving feature of the present level set method. Hence, the final design is properly connected and can be monolithic. The present geometric deformation constrained level set method may thus be more effective to generate reliable monolithic designs.

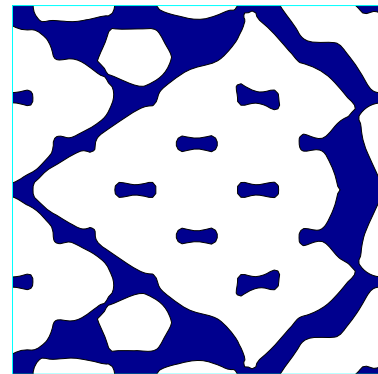
## 5 Conclusions

A geometric deformation constrained level set method is proposed for robust and effective shape

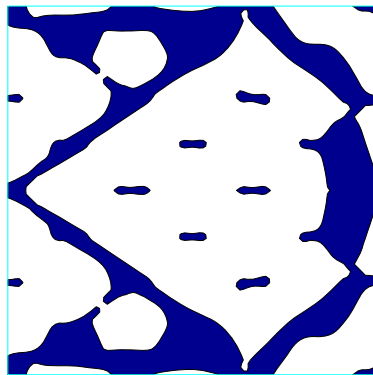
and/or topology optimization. The present level set method is first implemented to capture the motion of the free boundary of a structure to obtain an exploratory move at each time. Stable and smooth level set evolution with high accuracy can be achieved due to the appropriately chosen finite difference ENO scheme, extension velocity method, reinitialization and timestep size. Existence of solutions can be reached due to the present edge smoothing filtering on the extension velocities. Furthermore, the structural connectivity and/or structural topology can be explicitly taken as geometric deformation constraints on the resulting design, which may be well identified by an image-processing-based connected components labeling technique due to the present discrete 0-1 approximation of the design and the 4-neighborhood connectivity measure. Any violation on the geometric deformation constraints would disable the use of the exploratory move as the actual move and lead to further identification of the binary images of the designs before and after the move. The removed components crucial to structural connectivity and/or topology preserving can be further identified using the connected components labeling technique. The crucial components are recovered in the resulting design to preserve the structural connectivity and/or topology and the decrease of the objective function in structural shape and/or topology optimization can be well maintained because of the steep-



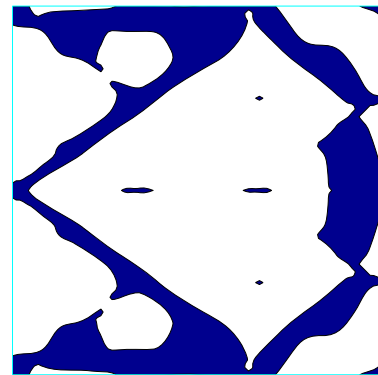
(a) Initial design



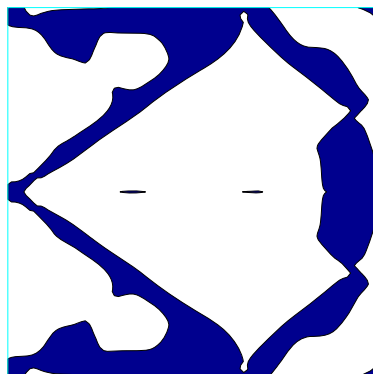
(b) Design 200



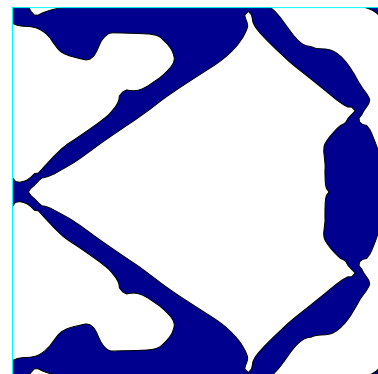
(c) Design 400



(d) Design 600



(e) Design 800



(f) Final design (design 1000)

Figure 19: Evolution history of a final design for the inverter mechanism using the present level set method ( $k_{in} = k_{out} = 0.008$ ).



Figure 20: FE Model of the final design for the inverter mechanism.

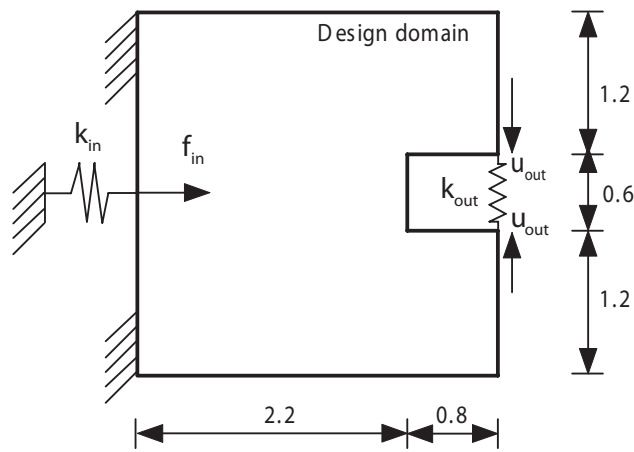


Figure 21: Gripper mechanism design problem.

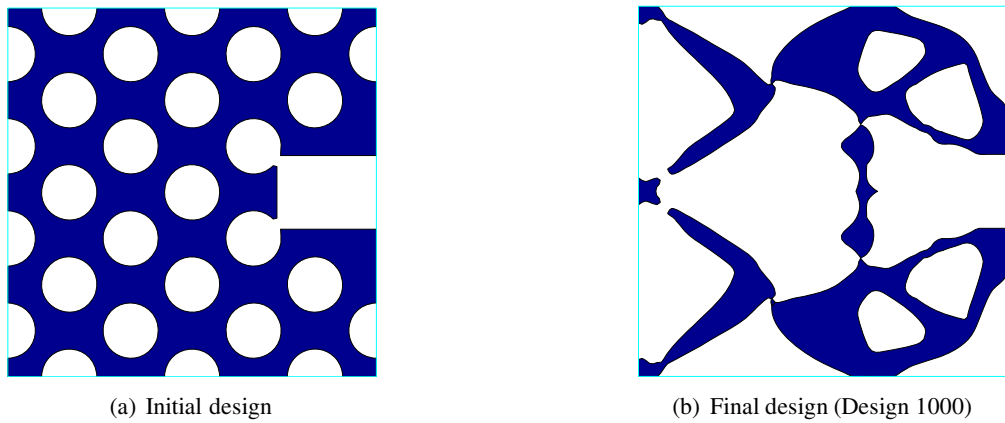


Figure 22: Optimal design for the gripper mechanism using a conventional level set method ( $k_{in} = k_{out} = 0.002$ ).

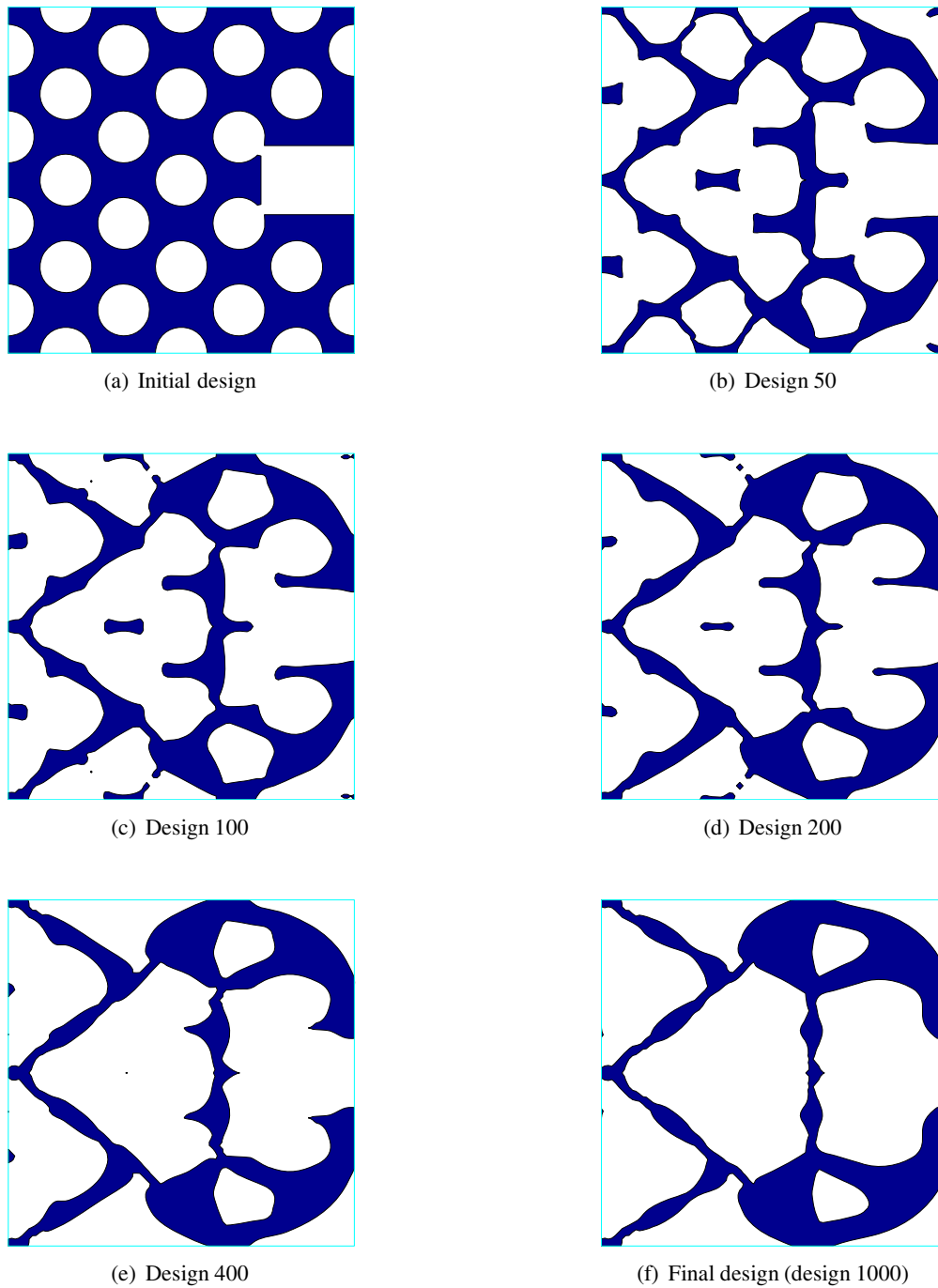


Figure 23: Evolution history of a final design for the gripper mechanism using the present level set method ( $k_{in} = k_{out} = 0.002$ ).

est gradient method. The geometric deformation constraints are thus imposed during the level set evolution and the resulting design after the actual move can be reliable and properly connected. The mere boundary-based shape optimization may be allowed for and simultaneous shape and topology optimization may become more robust. A bisectioning algorithm is used to handle the volume constraint to guarantee a feasible design since the fluctuations of the total volume can be effectively prevented. The present level set method may be structural connectivity and/or topology preserving and volume conservative to generate monolithic feasible designs. Numerical examples show the distinctive effectiveness of the present level set method in minimum compliance design and compliant mechanism design. It is suggested that a level set method with geometric deformation constraints may be more powerful and robust in the field of structural optimization.

## References

- Allaire, G.** (2001): *Shape Optimization by the Homogenization Method*. Springer, New York.
- Allaire, G.; de Gournay, F.; Jouve, F.; Toader, A. M.** (2005): Structural optimization using topological and shape sensitivity via a level set method. *Control and Cybernetics*, vol. 34, no. 1, pp. 59–80.
- Allaire, G.; Gournay, F. D.; Jouve, F.; Toader, A.-M.** (2004): Structural optimization using topological and shape sensitivity via a level set method. Internal report 555, Ecole Polytechnique, France, 2004.
- Allaire, G.; Jouve, F.; Toader, A.-M.** (2002): A level-set method for shape optimization. *C. R. Acad. Sci. Paris, Serie I*, vol. 334, pp. 1125–1130.
- Allaire, G.; Jouve, F.; Toader, A.-M.** (2004): Structural optimization using sensitivity analysis and a level-set method. *Journal of Computational Physics*, vol. 194, pp. 363–393.
- Amstutz, S.; Andrä, H.** (2006): A new algorithm for topology optimization using a level-set method. *Journal of Computational Physics*, vol. 216, pp. 573–588.
- Atluri, S. N.; Shen, S. P.** (2002): *The meshless local Petrov-Galerkin (MLPG) method*. Tech. Science Press, Forsyth, GA.
- Belytschko, T.; Black, T.** (1999): Elastic crack growth in finite elements with minimal remeshing. *International Journal for Numerical Methods in Engineering*, vol. 45, no. 5, pp. 601–620.
- Belytschko, T.; Xiao, S. P.; Parimi, C.** (2003): Topology optimization with implicit functions and regularization. *International Journal for Numerical Methods in Engineering*, vol. 57, no. 8, pp. 1177–1196.
- Bendsøe, M. P.; Sigmund, O.** (2003): *Topology Optimization: Theory, Methods and Applications*. Springer-Verlag, Berlin.
- Burger, M.; Hackl, B.; Ring, W.** (2004): Incorporating topological derivatives into level set methods. *Journal of Computational Physics*, vol. 194, pp. 344–362.
- Chang, F.; Chen, C.-J.; Lu, C.-J.** (2004): A linear-time component-labeling algorithm using contour tracing technique. *Computer Vision and Image Understanding*, vol. 93, no. 2, pp. 206–220.
- Chen, S. K.; Wang, M. Y.; Wang, S. Y.; Xia, Q.** (2005): Optimal synthesis of compliant mechanisms using a connectivity preserving level set method. In *ASME Proceedings of IDETC/CIE 2005*, pp. DETC2005–84748, Long Beach, California, USA.
- Han, X.; Xu, C. Y.; Prince, J. L.** (2003): A topology preserving level set method for geometric deformable models. *IEEE Transactions on Pattern Analysis and Machine Intelligence*, vol. 25, no. 6, pp. 755–768.
- Haug, E. J.; Choi, K. K.; Komkov, V.** (1986): *Design Sensitivity Analysis of Structural Systems*. Academic Press, Orlando.

- Jahne, B.** (1997): *Digital Image Processing - Concepts, Algorithms, and Scientific Applications*. Springer-Verlag, Berlin, 4th edition.
- Mechkour, H.; Jouve, F.; Bidard, C.; Rotinat-Libersa, C.** (2006): Optimal design of compliant mechanisms by level set and flexible building methods. In *Proceedings of IDETC/CIE 2006*, pp. DETC2006-99359, Philadelphia, Pennsylvania, USA. ASME 2006 International Design Engineering Technical Conferences & Computers and Information in Engineering Conference.
- Mei, Y. L.; Wang, X. M.** (2004): A level set method for structural topology optimization and its applications. *Advances in Engineering Software*, vol. 35, pp. 415-441.
- Norato, J.; Haber, R.; Tortorelli, D.; Bendsøe, M. P.** (2004): A geometry projection method for shape optimization. *International Journal for Numerical Methods in Engineering*, vol. 60, no. 14, pp. 2289-2312.
- Osher, S.; Fedkiw, R. P.** (2001): Level set methods: An overview and some recent results. *Journal of Computational Physics*, vol. 169, pp. 463-502.
- Osher, S.; Paragios, N.** (2003): *Geometric Level Set Methods in Imaging, Vision, and Graphics*. Springer-Verlag, New York.
- Osher, S.; Santosa, F.** (2001): Level-set methods for optimization problems involving geometry and constraints: Frequencies of a two-density inhomogeneous drum. *Journal of Computational Physics*, vol. 171, pp. 272-288.
- Osher, S.; Sethian, J. A.** (1988): Front propagating with curvature dependent speed: Algorithms based on Hamilton-Jacobi formulations. *Journal of Computational Physics*, vol. 78, pp. 12-49.
- Osher, S. J.; Fedkiw, R. P.** (2002): *Level Set Methods and Dynamic Implicit Surfaces*. Springer-Verlag, New York.
- Rahmatalla, S.; Swan, C. C.** (2005): Sparse monolithic compliant mechanisms using continuum structural topology optimization. *International Journal for Numerical Methods in Engineering*, vol. 62, pp. 1579-1605.
- Sethian, J. A.** (1999): *Level Set Methods and Fast Marching Methods*. Cambridge Monographs on Applied and Computational Mathematics. Cambridge University Press, Cambridge, UK, 2nd edition.
- Sethian, J. A.; Wiegmann, A.** (2000): Structural boundary design via level set and immersed interface methods. *Journal of Computational Physics*, vol. 163, no. 2, pp. 489-528.
- Sigmund, O.** (2001): A 99 line topology optimization code written in MATLAB. *Structural and Multidisciplinary Optimization*, vol. 21, no. 2, pp. 120-127.
- Sokolowski, J.; Źochowski, A.** (2001): Topological derivatives of shape functionals for elasticity systems. *Mechanics of Structures and Machines*, vol. 29, no. 3, pp. 331-349.
- Sokolowski, J.; Zolesio, J.-P.** (1992): Introduction to shape optimization: shape sensitivity analysis. In *Springer Series in Computational Mathematics*, volume 10. Springer, Berlin, Germany.
- Strouboulis, T.; Copps, K.; Babuska, I.** (2001): The generalized finite element method. *Computer Methods in Applied Mechanics and Engineering*, vol. 190, pp. 4081-4193.
- Tsai, R.; Osher, S.** (2003): Level set methods and their applications in image science. *Communications in Mathematical Sciences*, vol. 1, no. 4, pp. 623-656.
- Vese, L. A.; Chan, T. F.** (2002): A multiphase level set framework for image segmentation using the Mumford and Shah model. *International Journal of Computer Vision*, vol. 50, pp. 271-293.
- Wang, M. Y.; Chen, S.; Wang, X.; Mei, Y.** (2005): Design of multimaterial compliant mechanisms using level-set methods. *ASME Journal of Mechanical Design*, vol. 127, pp. 941-956.

**Wang, M. Y.; Wang, S. Y.** (2005): Bilateral filtering for structural topology optimization. *International Journal for Numerical Methods in Engineering*, vol. 63, no. 13, pp. 1911–1938.

**Wang, M. Y.; Wang, X.** (2004): PDE-driven level sets, shape sensitivity and curvature flow for structural topology optimization. *CMES: Computer Modeling in Engineering & Sciences*, vol. 6, no. 4, pp. 373–396.

**Wang, M. Y.; Wang, X.** (2005): A level-set based variational method for design and optimization of heterogeneous objects. *Computer-Aided Design*, vol. 37, pp. 321–337.

**Wang, M. Y.; Wang, X.; Guo, D.** (2003): A level set method for structural topology optimization. *Computer Methods in Applied Mechanics and Engineering*, vol. 192, pp. 227–246.

**Wang, M. Y.; Wang, X.; Guo, D.** (2004): Structural shape and topology optimization in a level set method based framework of region representation. *Structural and Multidisciplinary Optimization*, vol. 27, pp. 1–19.

**Wang, M. Y.; Wang, X. M.** (2004): “Color” level sets: A multi-phase method for structural topology optimization with multiple materials. *Computer Methods in Applied Mechanics and Engineering*, vol. 193, no. 6–8, pp. 469–496.

**Wang, S. Y.; Lim, K. M.; Khoo, B. C.; Wang, M. Y.** (2007): An extended level set method for shape and topology optimization. *Journal of Computational Physics*, vol. 221, no. 1, pp. 395–421.

**Wang, S. Y.; Tai, K.; Wang, M. Y.** (2006): An enhanced genetic algorithm for structural topology optimization. *International Journal for Numerical Methods in Engineering*, vol. 65, no. 1, pp. 18–44.

**Wang, S. Y.; Wang, M. Y.** (2006): A moving superimposed finite element method for structural topology optimization. *International Journal for Numerical Methods in Engineering*, vol. 65, no. 11, pp. 1892–1922.

**Wang, S. Y.; Wang, M. Y.** (2006): Radial basis functions and level set method for structural topology optimization. *International Journal for Numerical Methods in Engineering*, vol. 65, no. 12, pp. 2060–2090.

**Wang, S. Y.; Wang, M. Y.** (2006): Structural shape and topology optimization using an implicit free boundary parametrization method. *CMES: Computer Modeling in Engineering & Sciences*, vol. 13, no. 2, pp. 119–147.

**Yin, L.; Ananthasuresh, G. K.** (2003): Design of distributed compliant mechanisms. *Mechanics Based Design of Structures and Machines*, vol. 31, no. 2, pp. 151–179.

**Zhou, S.; Wang, M. Y.** (2006): 3D multi-material structural topology optimization with the generalized Cahn-Hilliard equations. *CMES: Computer Modeling in Engineering & Sciences*, vol. 16, no. 2, pp. 83–102.

